*Korean J Physiol Pharmacol*
*Vol 12: 337-342, December, 2008*

# Diversity of Ion Channels in Human Bone Marrow Mesenchymal Stem Cells from Amyotrophic Lateral Sclerosis Patients

**Kyoung Sun Park[1], Mi Ran Choi[1], Kyoung Hwa Jung[1], SeungHyun Kim[2], Hyun Young Kim[2], Kyung Suk Kim[3], Eun-Jong Cha[4], Yangmi Kim[5,*], and Young Gyu Chai[1,†]**

*[1]Division of Molecular and Life Sciences, Hanyang University, Ansan, 426-791, [2]Department of Neurology, Hanyang University Hospital, Seoul 133-792, [3]Bioengineering Institute, CoreStem Inc., Seoul 133-822, [4]Department of Biomedical Engineering, College of Medicine, Chungbuk National University, Cheongju 361-763, [5]Department of Physiology, College of Medicine, Chungbuk National University, Cheongju 361-763, Korea*

**Human bone marrow mesenchymal stem cells (hBM-MSCs) represent a potentially valuable cell type for clinical therapeutic applications. The present study was designed to evaluate the effect of long-term culturing (up to $10^{th}$ passages) of hBM-MSCs from eight individual amyotrophic lateral sclerosis (ALS) patients, focusing on functional ion channels. All hBM-MSCs contain several MSCs markers with no significant differences, whereas the distribution of functional ion channels was shown to be different between cells. Four types of $K^+$ currents, including noise-like $Ca^{+2}$-activated $K^+$ current ($IK_{Ca}$), a transient outward $K^+$ current ($I_{to}$), a delayed rectifier $K^+$ current ($IK_{DR}$), and an inward-rectifier $K^+$ current ($K_{ir}$) were heterogeneously present in these cells, and a TTX-sensitive $Na^+$ current ($I_{Na,TTX}$) was also recorded. In the RT-PCR analysis, *Kv1.1, heag1, Kv4.2, Kir2.1, MaxiK,* and *hNE-Na* were detected. In particular, $I_{Na,TTX}$ showed a significant passage-dependent increase. This is the first report showing that functional ion channel profiling depend on the cellular passage of hBM-MSCs**

**Key Words: Bone marrow, Stem cells, Functional ion channels, Tetrodotoxin-sensitive $Na^+$ current, Passage-dependency**

## INTRODUCTION

Clinical trials evaluating hBM-MSCs have demonstrated the ability of these cells to repair the site of tissue damage in cartilage fractures (Hannouche et al, 2007), metabolic diseases (Karnieli et al, 2007), amyotrophic lateral sclerosis (Mazzini et al, 2006), and myocardial infarction (Tomita et al, 1999; Orlic et al, 2001).

The original report on MSCs by Friedenstein et al. (1974) demonstrated that the MSCs can be amplified to approximately 30 doublings in culture while maintaining the ability of differentiate into osteoblasts, chondrocytes, and adipocytes. However, DiGirolamo CM et al and other researchers have shown that hBM-MSCs cultured *in vitro* display a tendency to lose their proliferative potential, homing capability, and multipotentiality (Banfi et al, 2000; Rombouts & Ploemacher, 2003; Stenderup et al, 2003). Indeed, some reports have demonstrated that telomere length changes after each cell cycle division in BM-MSCs (Baxter et al, 2004; Bonab et al, 2006).

Ion channels are widely expressed in proliferative cells which can modulate the proliferation of cells by affecting the cell cycle (MacFarlane & Sontheimer, 2000; Ouadid-Ahidouch et al, 2004; Biagiotti et al, 2006). Recent studies from our group and others have demonstrated that multifunctional ion channels are heterogeneously expressed in various species of MSCs (Li et al, 2005; Deng et al, 2006; Li et al, 2006; Park et al, 2007; Tao et al, 2007). The present study was designed to investigate changes in the expression patterns of passage-dependent ion channels in undifferentiated hBM-MSCs from ALS patients using a whole cell patch clamp technique and real time RT-PCR.

## METHODS

### *Study population and hBM-MSC cultures*

The donors were eight ALS patients: six males aged 35~63 years and two females aged 61 years. All patients signed informed written consent forms. This study was approved by the Institutional Review Board at Hanyang University (Seoul, Korea).

To isolate hBM-MSCs, bone marrow was obtained from the iliac crests of ALS patients. Mononuclear cells were isolated using a density gradient (Sigma-Aldrich, St. Louis,

*Corresponding to: Yangmi Kim, Department of Physiology, College of Medicine and Medical Research Institute, Chungbuk National University, Cheongju 361-763, Korea. (Tel) 82-43-261-2861, (Fax) 82-43-272-1603, (E-mail) yangmik@chungbuk.ac.kr
†Co-corresponding author: Young Gyu Chai, Division of Molecular and Life Sciences, Hanyang University, Ansan 426-791, Korea. (Tel) 82-31-400-5513, (Fax) 82-31-406-6316, (E-mail) ygchai@hanyang.ac.kr

**ABBREVIATIONS:** hBM-MSCs, Human bone marrow mesenchymal stem cells; ALS, amyotrophic lateral sclerosis; $IK_{Ca}$, $Ca^{2+}$-activated $K^+$ current; $I_{to}$, transient outward $K^+$ current; $IK_{DR}$, delayed rectifier $K^+$ current; $K_{ir}$, inward-rectifier $K^+$ current; $I_{Na,TTX}$, TTX-sensitive $Na^+$ current.

MO, density 1.077 g/mL). After 3 days, non-adherent cells were removed and the culture medium was changed twice per week. During *in vitro* passage (up to $10^{th}$), the cells were expanded for successive passages until they were confluent.

### *Flow cytometry analysis and differentiation of hBM-MSCs*

Cells were analyzed by flow cytometry (FACSCalibur A, BD Biosciences, San Jose, CA), as previously described (Park et al, 2007). Cell-surface epitopes were evaluated using anti-human antibodies: CD29-fluorescein isothiocyanate (FITC), CD105-FITC, HLA-DR-FITC, CD34-phycoerythrin (PE), CD45-PE (Serotec, Oxford, UK), CD44-FITC (DakoCytomation, Glostrup, Denmark), and CD73-PE (BD Bioscience, Franklin Lakes, NJ). Mouse isotype antibodies (FITC, PE) served as controls (Serotec). Adipogenic and osteogenic differentiations were performed according to the manufacturer's instructions using a Human Mesenchymal Stem Cell Functional Identification Kit (R&D systems, Minneapolis, MN).

### *Electrophysiological recordings and chemicals*

The hBM-MSCs from eight samples were used for the ionic current studies using a whole cell patch clamp technique, as previously described (Park et al, 2007). The experiments were conducted at room temperature. Four-aminopyridine (4-AP), verapamil, and tetraethylammonium (TEA) were ordered from Sigma-Aldrich and tetrodotoxin (TTX) and iberiotoxin was purchased from Tocris (Ellisville, MO).

### *RT-PCR and Quantitative RT - PCR*

The hBM-MSCs from three samples were used for RT-PCR analysis performed according to a previously described procedure (Park et al, 2007). The forward and reverse PCR oligonucleotide primers chosen to amplify the cDNA are listed in Table 1. The cDNA at 2 $\mu$l aliquots was

**Table 1.** List of ion channel primers used for RT-PCR

| Gene | Acc. No. | Forward primer (5'-3') | Reverse primer (5'-3') |
|---|---|---|---|
| Kv1.1 | L02750 | CCATCATTCCTTATTTCATCAC | CTCTTCCCCCTCAGTTTCTC |
| Heag1 | AJ001366 | TGGATTTTGCAAGCTGTCTG | GAGTCTTTGGTGCCTCTTGC |
| Kv4.2 | AJ010969 | ATCTTCCGCCACATCCTGAA | GATCCGCACGGCACTGTTTC |
| Kir2.1 | L36069 | GACCTGGAGACGGACGAC | AGCCTGGAGTCTGTCAAAGTC |
| MaxiK | U11058 | ACAACATCTCCCCCAACC | TCATCACCTTCTTTCCAATTC |
| hNE-Na | X82835 | GCTCCGAGTCTTCAAGTTGG | GGTTGTTTGCATCAGGGTCT |
| SCN5A | M77235 | CCTAATCATCTTCCGCATCC | TGTTCATCTCTCTGTCCTCATC |
| $\beta$-actin | NM001101 | TCATGTTTGAGACCTTCAA | GTCTTTGCGGATGTCCACG |

Abbreviations: Acc. No., accession number.

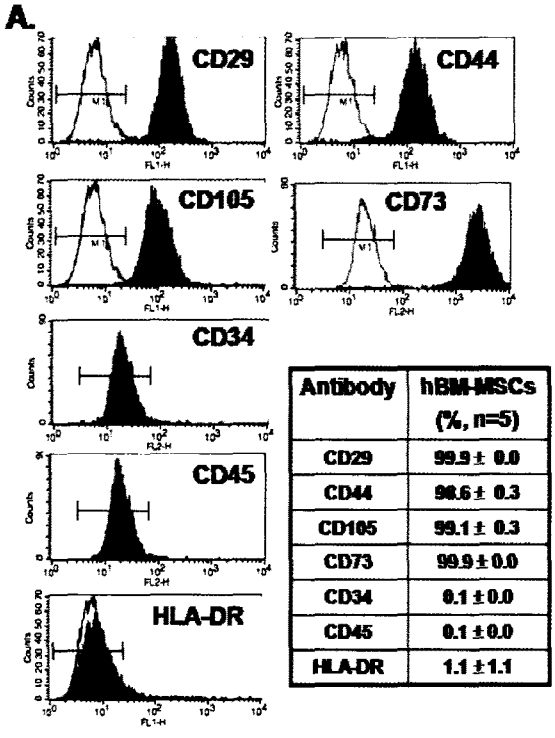


Fig. 1. Characterization of hBM-MSCs. (A) Flow cytometry analysis showing that hBM-MSCswere positive for CD29, CD44, CD105, and CD73 and were negative for CD34, CD45, and HLA-DR. The table shows mean values (%). (B) hBM-MSCs expressed markers for OPN, LIFR, ABCG2, CXCR4, CD44, collagen X, collagen1 and alpha1. The hBM-MSCs RNAs were obtained from different donors (I and II, n=4) (C) Differentiation capacity of hBM-MSCs to adipocytes (upper) and osteoblasts (lower). 200× magnification.

amplified by a DNA thermal cycler (Bio-Rad Laboratories, Hercules, CA) in a 25 $\mu$l reaction mixture; the mixture was annealed at 50~61°C (1 minute), extended at 72°C (2 minutes), and denatured at 95°C (45 seconds) for 30~35 cycles. Quantitative RT-PCR was performed with the 7,500 fast quantitative PCR System (Applied Biosystems, Foster City, CA) using SYBR Green master mix (Takara Bio Inc., Shiga, Japan). During each cycle, the accumulation of PCR products was detected by monitoring the increase in reporter dye fluorescence from dsDNA-bound SYBR Green. GAPDH was used as a control.

### *Data analysis and statistics*

Nonlinear-fitting programs (Origin, Northampton, MA) were used and statistical results are presented as mean± standard error of the mean (SEM). Paired and unpaired Student's *t*-tests were used as appropriate to evaluate the statistical significance of differences between two groups of means. p-Values were considered to indicate statistical significance.

## RESULTS

### *Expression of stem cell markers and differentiation potential in hBM-MSCs*

MSCs-specific surface markers (Weiss et al, 2006) present on hBM-MSCs at the 4$^{th}$ and 7$^{th}$ passages were analyzed by flow cytometry (Fig. 1A). The cells were positive for integrin markers (CD29), adhesion molecules (CD44), and MSCs markers (CD105, CD73) and were negative for hematopoietic (CD34, CD45) and major histocompatibility antigen (HLA-DR). We performed RT-PCR analysis to evaluate the expression of stem cell-specific genes. As shown in Fig. 1B, hBM-MSCs expressed markers of the osteogenic state (OPN), undifferentiated state (LIFR, ABCG2), mesoderm state (CXCR4, CD44, collagen X), and extracellular matrix molecules (collagen1, alpha1). The expression pattern of surface proteins and genes on our hBM-MSCs preparations was consistent those obtained by the Cambrex Corporation (Park et al, 2007) and the results indicate that these cells are primitive MSC populations. There were no significant differences among samples from the eight individual donors or among cells from different passages. To evaluate the differentiation capacity of hBM-MSCs, the cells were cultured in adipogenic and osteogenic medium for 3 weeks. Fig. 1C shows the capacity of hBM-MSCs to differentiate into adipocytes (upper) and osteoblasts (lower).

### *Functional ion channel recordings in hBM-MSCs by whole cell patch clamp*

Whole cell patch clamp recordings were made from the 2$^{nd}$~10$^{th}$ passages obtained from eight samples. Membrane currents were elicited by 300 ms voltage steps between −120 and +100 mV from a holding potential of −80 mV in hBM-MSCs, as illustrated in Fig. 2. The hBM-MSCs displayed four types of $K^+$ currents: $IK_{DR}$, $IK_{Ca}$, $I_{to}$, and $K_{ir}$. The $IK_{Ca}$ usually coexisted with $IK_{DR}$ in most hBM-MSCs (462 out of 476 cells, 97.1%, Fig. 2A) and was effectively inhibited by treatment with 5 mM TEA (Fig. 3A). $I_{to}$ was detected in only 3.7% of the cells (18 out of 476 cells, Fig. 2B). $I_{to}$ was substantially inhibited by 300 $\mu$M 4-AP, but remained unaffected by TEA (Fig. 3A, middle). Another

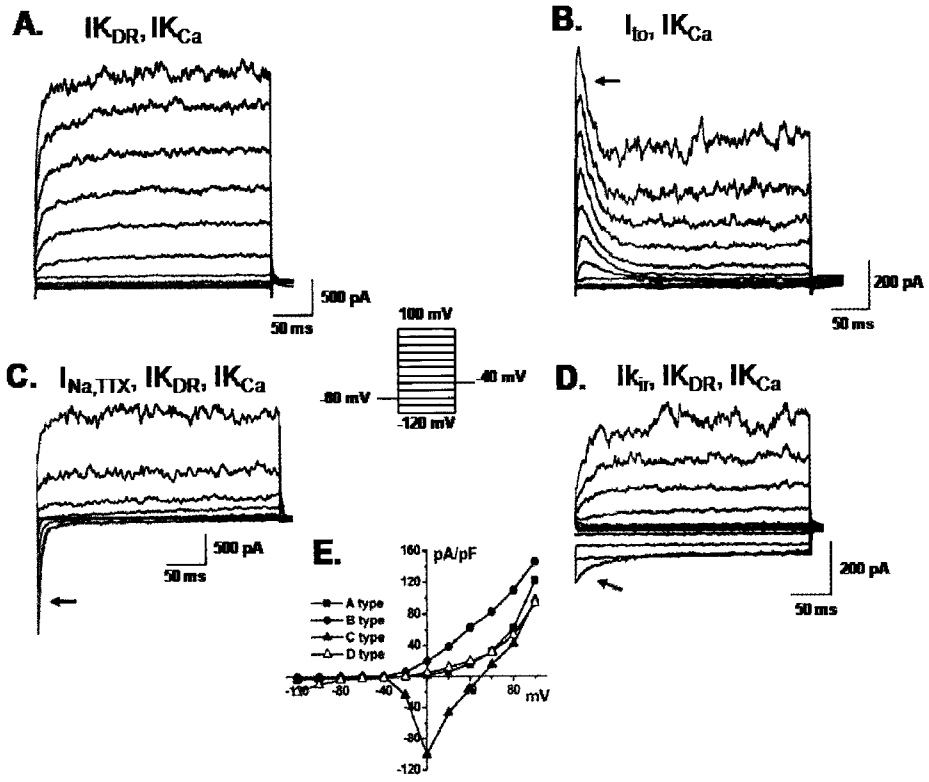


Fig. 2. Different patterns of membrane currents recorded in hBM-MSCs. Current traces elicited by the voltage step (inset) in hBM-MSCs. (A) a slowly activating current similar to $IK_{DR}$ at potentials from +20 to +100 mV that coexisted with $IK_{Ca}$. (B) $I_{to}$ (arrow) with $IK_{Ca}$. (C) $I_{Na,TTX}$ (arrow) with $IK_{DR}$ and $IK_{Ca}$. (D) $IK_{ir}$ (arrow) with $IK_{DR}$ and $IK_{Ca}$. (E) Current-voltage relationships were plotted from A, B, C and D.

type of $K^+$ current, inward-rectifier $K^+$ current, were evoked using a ramp voltage from −150 to +60 mV for 400 ms at a holding potential of 0 mV (4.4%, 21 out of 476 cells, Fig. 2D, arrow). The *I-V* relationships were plotted by ramp voltage-induced inward currents against membrane potentials in bath solutions containing 5, 15, 30, 75, and 150 mM $K^+$, as indicated (Fig 3C). The reversal potential was positively shifted as external $K^+$ concentration increased, suggesting that $K^+$ induces this current. The plot of the reversal potential as a function of $[K^+]_o$ showed that the slope was 66.04±5.55 mV/10-fold change in $[K^+]_o$ (Fig. 3C right panel, n=6). The current was blocked in a dose-dependent manner by $Ba^{2+}$, a $K_{ir}$-specific blocker ($IC_{50}$ at −100 mV; 162.2±22.2 $\mu$M).

A $Na^+$ current was found in a small population of cells using our experimental voltage protocols for outward currents (11.5%, 55 out of 476 cells, Fig. 2C, arrow). This inward current was blocked by TTX ($I_{Na,TTX}$, Fig. 3B). Interestingly, $I_{Na,TTX}$ was also blocked by verapamil (Fig 3B right panel), a $Ca^{2+}$ channel antagonist but nifedipine, a L-type $Ca^{2+}$ channel blocker, demonstrated no blocking effect (data not shown). These findings suggest that the current is a TTX-sensitive $Na^+$ current and is sensitive to verapamil.

### *Passage-dependent mRNA expression of ion channels in hBM-MSCs*

During the electrophysiological studies of hBM-MSCs ($2^{nd}$ ~$10^{th}$ passages) from eight samples, we found that the recording rate of $Na^+$ currents, in particular, varied according to the passage number. Therefore, we investigated the mRNA levels present during different passages in three hBM-MSCs samples by RT-PCR and quantitative RT-PCR analysis. *MaxiK* for $IK_{Ca}$, *Kv4.2* for $I_{to}$, *Kv1.1* and *heag1* for $IK_{DR}$, *hNE-Na* for $I_{Na,TTX}$, and *Kir2.1* for $K_{ir}$ were detected in hBM-MSCs (Fig. 4A). $\beta$-actin was used as the control. The gene expression levels of all channels were low at an early passage ($3^{rd}$), except for the *MaxiK* gene. Relative quantities of the *Kv1.1*, *Heag1*, and *Kir2.1* genes and *MaxiK* remain unchanged from the $5^{th}$ through the $9^{th}$ passage, but not *hNE-Na* (Fig. 4A). The "recording rate (%)" of $I_{Na,TTX}$ increased almost three-fold more in late passages compared to early passages based on whole cell patch configurations (Fig. 4B). The "recording rate (%)" of $I_{Na,TTX}$ was determined by the number of $Na^+$ current recordings by dividing the totally achieved of whole cell patch configurations. *MaxiK* gene levels (RQ) also displayed a visible change between passages, but the variation was not as extreme as that observed for the *hNE-Na* gene levels (RQ) by quantitative RT-PCR (n=3, each from three samples, Fig. 4C and 4D). Representative passage-dependent *hNE-Na* and *MaxiK* gene expression patterns (RT-PCR) from two different samples are displayed in the inset of Fig. 4C and 4D.

## DISCUSSION

In our study, all cells isolated from the BM of ALS patients exhibited typical MSC characteristics (morphology, differentiation capacity, and expression of a typical set of surface proteins and genes). Each hBM-MSCs obtained from ALS patients showed a passage dependent gradual increase in $Na^+$ channel expression, which may provide additional information for autologous cell based therapy.

### *Comparisons of the distribution and function of ion channels in BM-MSCs*

Four types of $K^+$ current ($IK_{Ca}$, $IK_{DR}$, $I_{to}$ and $K_{ir}$) and one type of inward current ($I_{Na,TTX}$) were detected using the patch clamp technique in hBM-MSCs from ALS patients. This is the first study of channel expression in continuously passaged hBM-MSCs. The expression of multiple ion channels indicates possible functions of these different channels in the cellular physiological activity of hBM-MSCs. Deng et al reported that $IK_{DR}$ decreases during cell cycle progression in rat BM-MSCs, while $IK_{Ca}$ increases during pro-

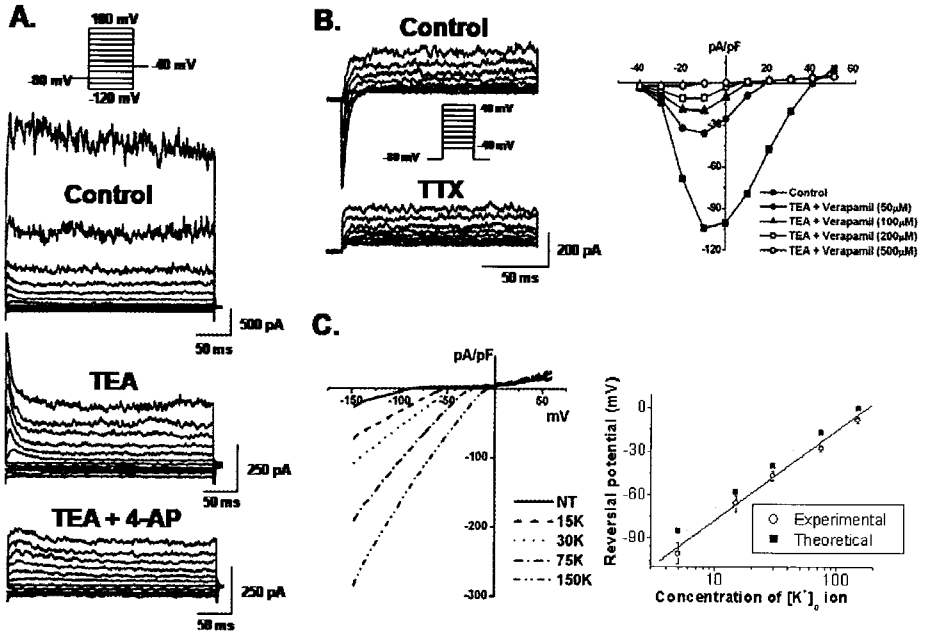


Fig. 3. Pharmacological effects of functional ion channels in hBM-MSCs. (A) Membrane currents were recorded in the presence of 10 mM TEA or co-application of TEA and 300 $\mu$M 4-AP. (B) $I_{Na,TTX}$ was continuously recorded under control conditions and in the presence of TTX. $I_{Na,TTX}$ was blocked by TTX (left panel) and also blocked by verapamil (right panel). (C) The *I-V* relationships of $K_{ir}$ were obtained by ramp voltage induced currents against membrane potentials in bath solutions containing 5, 15, 30, 75, and 150 mM $K^+$ as indicated (left panel). Reversal potentials from six patches were observed and plotted as a function of external $[K^+]$ concentrations (right panel). The dotted line represents the slope from the Nernst equation (slope, 58 mV/decade). Experimental values (O) were fitted by linear regression (slope, 66 mV/decade).

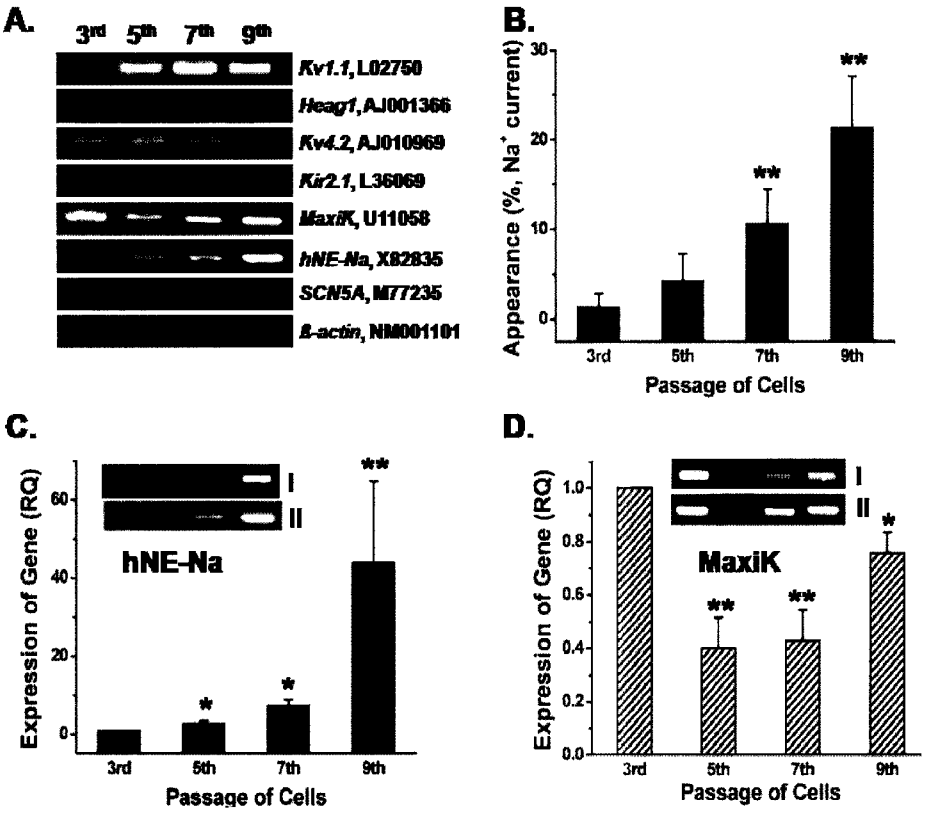


Fig. 4. Comparison of mRNA expression of ion channels between passages. (A) *Kv1.1, heag1* (for $IK_{DR}$), *Kv4.2* (for $I_{to}$), *Kir2.1* (for $K_{ir}$), *MaxiK* (for $IK_{Ca}$) and *hNE-Na* (for $I_{Na,TTX}$) were detected in hBM-MSCs, but not SCN5A (for TTX-resistant $I_{Na}$). *β-actin* was used as the control. (B) The "recording rate (%)" of $I_{Na,TTX}$ in various passage of hBM-MSCs. (C) Relative passage-dependent mRNA quantities of the *hNE-Na* gene by quantitative RT-PCR (n=3). The inset in Fig. 4C shows a representative result for the *hNE-Na* gene from two different samples. (D) Relative passage-dependent *MaxiK* gene expression levels in hBM-MSCs. Inset in Fig. 4D displays representative passage-dependent *MaxiK* channel gene expression patterns from two different samples. *$p<0.05$, **$p<0.005$ when compared with each 3rd passage group.

gression from the G1 to S phase (Deng et al, 2007). Other reports showed that inhibition of $K^+$ currents by treatment with $K^+$ channel blockers, TEA and clofilium, also inhibited the hMSCs proliferation (Balana et al, 2006). These reports suggest that ion channels may participate in the proliferation of stem cells.

### *Passage dependent increases in the expression of $Na^+$ channel in hBM-MSCs*

Voltage-gated $Na^+$ channels have been well known to be responsible for action potential initiation and propagation in excitable cells, including nerve, muscle, and cardiac cells. Therefore, the $Na^+$ channel may serve important functions during hBM-MSCs differentiation as it plays a distinct function in cardiac and neuronal cells. In the present study, we found that TTX-sensitive $Na^+$ current (responsible for *hNE-Na*) increased approximately three-fold during later compared to earlier cell passages, whereas a TTX-resistant $Na^+$ current (responsible for *SCN5A*) was not detected in our hBM-MSCs. This noticeable increase of the TTX-sensitive $Na^+$ current could lead to the activation of other channels via depolarization, which results from an influx of $Na^+$ ions into cells. Alternatively, the facilitated excitation of cells may serve to activate the intracellular signaling system. Taken together, the increment of $Na^+$ channels must be considered before using them. Based on the above results, we suggest that the TTX-sensitive $Na^+$ channel is significantly increased in during late passages of hBM-MSCs and that passage-dependent variation in functional ion channel expression might play a role in proliferation and/or differentiation.

Further investigation is needed to elucidate the role of $Na^+$ channels in the differentiation and proliferation of hBM-MSCs and to study the dependence of ion channel profiles on passages in the other mesenchymal stem cell lines.

## ACKNOWLEDGEMENTS

This work was supported by the Korea Research Foundation Grant funded by the Korean Government (MOEHRD, Basic Research Promotion Fund, KRF 2007-532-E00001) and by the Korea Science and Engineering Foundation (KOSEF) grant funded by the Korea government (MEST) (R11-2008-014-02001-0).

## REFERENCES

Balana B, Nicoletti C, Zahanich I, Graf EM, Christ T, Boxberger S, Ravens U. 5-Azacytidine induces changes in electrophysiological properties of human mesenchymal stem cells. *Cell Res* 16: 949–960, 2006

Banfi A, Muraglia A, Dozin B, Mastrogiacomo M, Cancedda R, Quarto R. Proliferation kinetics and differentiation potential of ex vivo expanded human bone marrow stromal cells: Implications for their use in cell therapy. *Exp Hematol* 28: 707–715, 2000

Baxter MA, Wynn RF, Jowitt SN, Wraith JE, Fairbairn LJ, Bellantuono I. Study of telomere length reveals rapid aging of human marrow stromal cells following in vitro expansion. *Stem Cells* 22: 675–682, 2004

Biagiotti T, D'Amico M, Marzi I, Di Gennaro P, Arcangeli A, Wanke E, Olivotto M. Cell renewing in neuroblastoma: electrophysiological and immunocytochemical characterization of stem cells and derivatives. *Stem Cells* 24: 443–453, 2006

Bonab MM, Alimoghaddam K, Talebian F, Ghaffari SH,

Ghavamzadeh A, Nikbin B. Aging of mesenchymal stem cell in vitro. *BMC Cell Biol* 7: 14, 2006

Deng XL, Lau CP, Lai K, Cheung KF, Lau GK, Li GR. Cell cycle-dependent expression of potassium channels and cell proliferation in rat mesenchymal stem cells from bone marrow. *Cell Prolif* 40: 656−670, 2007

Deng XL, Sun HY, Lau CP, Li GR. Properties of ion channels in rabbit mesenchymal stem cells from bone marrow. *Biochem Biophys Res Commun* 348: 301−309, 2006

Friedenstein AJ, Deriglasova UF, Kulagina NN, Panasuk AF, Rudakowa SF, Luria EA, Ruadkow IA. Precursors for fibroblasts in different populations of hematopoietic cells as detected by the in vitro colony assay method. *Exp Hematol* 2: 83−92, 1974

Hannouche D, Terai H, Fuchs JR, Terada S, Zand S, Nasseri BA, Petite H, Sedel L, Vacanti JP. Engineering of implantable cartilaginous structures from bone marrow-derived mesenchymal stem cells. *Tissue Eng* 13: 87−99, 2007

Karnieli O, Izhar-Prato Y, Bulvik S, Efrat S. Generation of insulin-producing cells from human bone marrow mesenchymal stem cells by genetic manipulation. *Stem Cells* 25: 2837−2844, 2007

Li GR, Deng XL, Sun H, Chung SS, Tse HF, Lau CP. Ion channels in mesenchymal stem cells from rat bone marrow. *Stem Cells* 24: 1519−1528, 2006

Li GR, Sun H, Deng X, Lau CP. Characterization of ionic currents in human mesenchymal stem cells from bone marrow. *Stem Cells* 23: 371−382, 2005

MacFarlane SN, Sontheimer H. Changes in ion channel expression accompany cell cycle progression of spinal cord astrocytes. *Glia* 30: 39−48, 2000

Mazzini L, Mareschi K, Ferrero I, Vassallo E, Oliveri G, Boccaletti R, Testa L, Livigni S, Fagioli F. Autologous mesenchymal stem cells: clinical applications in amyotrophic lateral sclerosis. *Neurol Res* 28: 523−526, 2006

Orlic D, Kajstura J, Chimenti S, Jakoniuk I, Anderson SM, Li B, Pickel J, McKay R, Nadal-Ginard B, Bodine DM, Leri A, Anversa P. Bone marrow cells regenerate infarcted myocardium. *Nature* 410: 701−705, 2001

Ouadid-Ahidouch H, Roudbaraki M, Delcourt P, Ahidouch A, Joury N, Prevarskaya N. Functional and molecular identification of intermediate-conductance Ca2+-activated K+ channels in breast cancer cells: association with cell cycle progression. *Am J Physiol Cell Physiol* 287: C125−134, 2004

Park KS, Jung KH, Kim SH, Kim KS, Choi MR, Kim Y, Chai YG. Functional expression of ion channels in mesenchymal stem cells derived from umbilical cord vein. *Stem Cells* 25: 2044−2052, 2007

Rombouts WJ, Ploemacher RE. Primary murine MSC show highly efficient homing to the bone marrow but lose homing ability following culture. *Leukemia* 17: 160−170, 2003

Stenderup K, Justesen J, Clausen C, Kassem M. Aging is associated with decreased maximal life span and accelerated senescence of bone marrow stromal cells. *Bone* 33: 919−926, 2003

Tao R, Lau CP, Tse HF, Li GR. Functional ion channels in mouse bone marrow mesenchymal stem cells. *Am J Physiol Cell Physiol* 293: C1561−1567, 2007

Tomita S, Li RK, Weisel RD, Mickle DA, Kim EJ, Sakai T, Jia ZQ. Autologous transplantation of bone marrow cells improves damaged heart function. *Circulation* 100 Suppl 19: II247−256, 1999

Weiss ML, Medicetty S, Bledsoe AR, Rachakatla RS, Choi M, Merchav S, Luo Y, Rao MS, Velagaleti G, Troyer D. Human umbilical cord matrix stem cells: preliminary characterization and effect of transplantation in a rodent model of Parkinson's disease. *Stem Cells* 24: 781−792, 2006